Measurements of the Photo-Induced Complex Permittivity of Si, Ge, and Te at 9 GHz

LI DING, MEMBER, IEEE, I. SHIH, THOMAS J. F. PAVLASEK, SENIOR MEMBER, IEEE, AND CLIFFORD H. CHAMPNESS

Abstract—**The photo-induced complex permittivity $\Delta\epsilon_r$ ($= \Delta\epsilon_r' - j\Delta\epsilon_r''$) of single crystal silicon, germanium, and tellurium samples was studied using a transmission microwave bridge method at frequencies of about 9 GHz. The measurements were made at temperatures in a range from 100 to 300 K over an optical wavelength range from about 0.6 to 1.4 μm for silicon, 0.8 to 2.0 μm for germanium, and 1.5 to 4.2 μm for tellurium. The incident monochromatic illumination was chopped at about 90 Hz. It was found that the spectral variation of $\Delta\epsilon_r'$ was similar to that for $\Delta\epsilon_r''$ over the wavelength ranges with the incident monochromatic light intensity in the order of 100 μw/cm^2. The spectral peaks (for Si and Ge samples) of both $\Delta\epsilon_r'$ and $\Delta\epsilon_r''$ were found to shift towards shorter wavelengths as the temperature was decreased. From the photo-induced complex permittivity results, the collision time of the free carriers was derived.**

I. Introduction

PHOTOCONDUCTIVITY measurement of semiconductors at microwave frequencies can provide useful information about the materials. Such measurements do not require electrical contacts for the passage of a current through the sample. Using a microwave resonator method, Cherkasov and Ionov [1] have studied the photoconductivity of amorphous selenium films at a frequency of about 10 GHz. Ionov *et al.* [2] have reported the photoconductivity results of organic dyes using the same method. Using a microwave reflection method, the photoconductivity in ZnS and CdS phosphors has been studied by Kalikstein *et al.* [3]. Recently, Collier *et al.* have reported the photoconductivity of CdS at a frequency of about 8 GHz [4]. In these measurements, the effect of incident light on the real part of the complex permittivity (photodielectric effect [5]) had not been considered. The measurements of the photodielectric effect due to the photo-induced free carriers may be used to determine the collision time and effective mass of carriers in the semiconductors. It seems also to be capable of providing a waveguide effect for submillimeter EM waves [6]. An optical control phase shifter [7] and a high-speed switch using picosecond photoconductivity [8] also have been reported for microwave signals. However, a practical experiment to observe the photodielectric and photoconductive effect at microwave frequencies seems to have been reported only once in the literature by Ionov [9]. In his study, the photoconductivity and the photodielectric effects of a sample were measured by using a cavity method at a frequency of about 10 GHz. In the present work, a microwave technique to determine very small changes of the photo-induced complex permittivity of semiconductors has been investigated. Permittivity measurements have been made on silicon, germanium, and tellurium samples under monochromatic optical illumination.

The collision time of free carriers in single-crystal germanium and tellurium samples has been studied previously by complex permittivity measurements at microwave frequencies [10]–[12]. In such experiments, the complex permittivity of the sample was measured over a temperature range. The carrier collision time can be derived from the measured complex permittivity data provided the values of magnitude of the real permittivity component (ϵ_{rl}') due to the lattice and the carrier concentration at a specific temperature are known. For semiconductors containing impurities and free carriers, it is often difficult to determine the exact real permittivity value which is required for the precise collision time determination. In the present work, the photo-induced complex permittivity measurements allow the collision time to be estimated from the ratio of the real and imaginary photo-induced permittivity values without knowing the absolute permittivity value.

II. Theory

A schematic diagram of the microwave bridge system used in the present study is shown in Fig. 1(a). When the microwave bridge is set from a balanced condition to an unbalanced one by adjusting the precision attenuator and phase shifter in the reference channel, the relation between the electric field vector in the reference channel ($\boldsymbol{E}_r$) and that in the sample channel ($\boldsymbol{E}_s$) is as follows:

$$\boldsymbol{E}_r = \boldsymbol{E}_s \times 10^{-A/20} e^{-j\phi} \tag{1}$$

where A is the attenuation change in decibels and ϕ is the phase change in radians in the reference channel. Now, assume there is a small change in both the attenuation and

Manuscript received January 5, 1983; revised August 23, 1983. This work was supported in part by the Natural Sciences and Engineering Research Council of Canada.

L. Ding is with the Radio Engineering Department, Chongqing University, Chongqing, Sichuan, People's Republic of China.

I. Shih, T. J. F. Pavlasek, and C. H. Champness are with the Department of Electrical Engineering, McGill University, 3480 University St., Montreal, PQ, H3A 2A7, Canada.

0018-9480/84/0200-0151$01.00 ©1984 IEEE

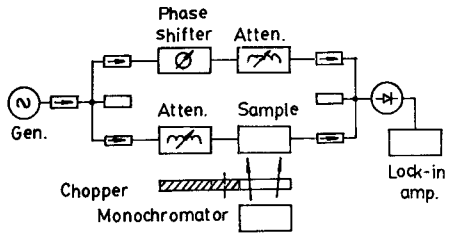

(a)

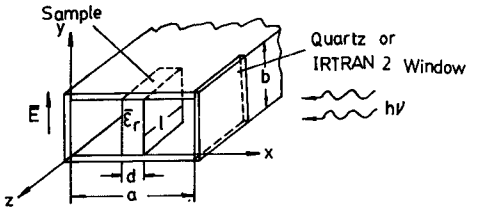

(b)

Fig. 1. (a) A schematic diagram of the microwave bridge system used for measurements. Gen.: Varian VA-5080 Klystron, Phase shifter: HP model 885A, Atten.: HP model 382A, Diode: KEMTRON IN23D, Lock-in amp.: Princeton Applied Research model 124A, Monochromator: Beckman model 2400. (b) Sample holder waveguide with a 'window' for external illumination.

phase shift of the EM wave in the sample channel due to the external illumination of the sample; then there will be a corresponding change in the electric field vectors in the E- and H-arm of the hybrid junction as shown in Fig. 2. From Fig. 2, the following equations which relate the change in both the attenuation (ΔA_s) and phase shift ($\Delta\phi_s$), due to the external illumination, to the resultant electric field change in the E-arm (ΔE_e) and H-arm (ΔE_h) can be derived as follows [13]:

$$\Delta A_s = -20\log\left(1+\frac{\Delta E_s}{E_s}\right) \quad \text{(dB)} \tag{2}$$

$$\begin{aligned}\Delta\phi_s = {} & \left(2\times 10^{-A/20}\sin\phi\right)^{-1} \\ & \cdot\Big[\left(1+10^{-A/20}\cos\phi\right) \\ & \cdot\left(1+10^{-A/10}-2\times 10^{-A/20}\cos\phi\right)^{1/2}\frac{\Delta E_e}{E_s} \\ & -\left(1-10^{-A/20}\cos\phi\right)\left(1+10^{-A/10}\right. \\ & \left.+2\times 10^{-A/20}\cos\phi\right)^{1/2}\frac{\Delta E_h}{E_s}\Big] \quad \text{(rad)}\end{aligned} \tag{3}$$

where

$$\begin{aligned}\frac{\Delta E_s}{E_s} = \frac{1}{2}\Big[& \left(1+10^{-A/10}-2\times 10^{-A/20}\cos\phi\right)^{1/2}\frac{\Delta E_e}{E_s} \\ & +\left(1+10^{-A/10}+2\times 10^{-A/20}\cos\phi\right)^{1/2}\frac{\Delta E_h}{E_s}\Big]\end{aligned} \tag{4}$$

and E_s is the electric field magnitude in the sample channel.

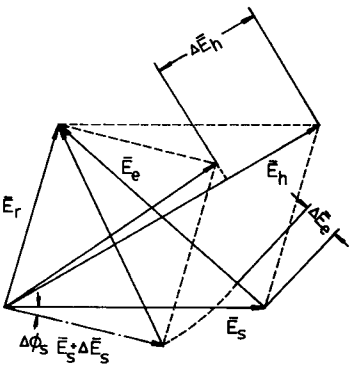

Fig. 2. Vector relation between E_e, E_h, E_r, and E_s.

The complex relative permittivity change of the sample due to the external illumination can then be calculated from the obtained ΔA_s and $\Delta\phi_s$ by using a perturbation method as described below.

For the partially filled waveguide shown in Fig. 1(b), we may obtain the following equation using the perturbation method [14]:

$$\gamma-\gamma_0 = \frac{j\omega\epsilon_0\int_0^{d/2}\int_0^{b}(\epsilon_r-1)\boldsymbol{E}\cdot\boldsymbol{E}_0^*\,dx\,dy}{\int_0^{a/2}\int_0^{b}\left[\boldsymbol{E}_0^*\times\boldsymbol{H}+\boldsymbol{E}\times\boldsymbol{H}_0^*\right]\cdot\boldsymbol{k}\,dx\,dy} \tag{5}$$

where

$$\boldsymbol{E}_0 = \boldsymbol{E}_0(x,y)e^{-\gamma_0 z}$$
$$\boldsymbol{H}_0 = \boldsymbol{H}_0(x,y)e^{-\gamma_0 z}$$

are the unperturbed fields (with sample in the waveguide), and where

$$\boldsymbol{E} = \boldsymbol{E}(x,y)e^{-\gamma z}$$
$$\boldsymbol{H} = \boldsymbol{H}(x,y)e^{-\gamma z}$$

are the perturbed fields (with sample in the waveguide). Here, $\boldsymbol{E}_0^*$ and $\boldsymbol{H}_0^*$ are the conjugates of the $\boldsymbol{E}_0$ and $\boldsymbol{H}_0$, $\epsilon_r = \epsilon_r' - j\epsilon_r''$ is the complex relative permittivity of the sample, and ϵ_0 is the dielectric constant of free space.

Integrating (5), we can obtain the following equations:

$$\epsilon_r' = \left(\frac{\lambda_0}{2\pi}\right)^2\left(\frac{a}{d}\right)\left(\beta^2-\beta_0^2-\alpha^2\right)+1 \tag{6}$$

$$\epsilon_r'' = \left(\frac{\lambda_0}{2\pi}\right)\left(\frac{a}{d}\right)(2\alpha\beta) \tag{7}$$

where λ_0 is the EM wavelength in free space, and where

$\beta_0\left(=\frac{2\pi}{\lambda_0}\sqrt{1-\left(\frac{\lambda_0}{2a}\right)^2}\right)$ phase constant of the empty waveguide in darkness,

$\alpha\left(=0.115\frac{\Delta A}{l}\right)$ attenuation constant of the partially filled waveguide in the dark,

$\beta\left(=\frac{\phi\times\pi}{180l}+\beta_0\right)$ phase constant of the partially filled waveguide in the dark.

From (6) and (7), the relative permittivity change, both the real and imaginary part, of the sample can be expressed

as follows:

$$\Delta\epsilon_r' = \frac{\partial\epsilon_r'}{\partial\alpha}\frac{\partial\alpha}{\partial A}\Delta A + \frac{\partial\epsilon_r'}{\partial\beta}\frac{\partial\beta}{\partial\phi}\Delta\phi = \frac{\lambda_0^2 a}{2\pi^2 dl}\left(\frac{\pi\beta}{180}\Delta\phi_s - 0.115\alpha\Delta A_s\right) \quad (8)$$

$$\Delta\epsilon_r'' = \frac{\partial\epsilon_r''}{\partial\alpha}\frac{\partial\alpha}{\partial A}\Delta A + \frac{\partial\epsilon_r''}{\partial\beta}\frac{\partial\beta}{\partial\phi}\Delta\phi = \frac{\lambda_0^2 a}{2\pi^2 dl}\left(\frac{\pi\alpha}{180}\Delta\phi_s + 0.115\beta\Delta A_s\right) \quad (9)$$

and

$$\Delta\epsilon_r = \Delta\epsilon_r' - j\Delta\epsilon_r''. \quad (10)$$

For a nondegenerate semiconductor with a free-carrier concentration n per unit volume, a classical permittivity equation can be derived [10] assuming a constant collision time (τ) for all the carriers:

$$\epsilon_r = \epsilon_r' - j\epsilon_r'' = \left[\epsilon_{rl}' - \frac{\sigma_0\tau}{\epsilon_0(1+\omega^2\tau^2)}\right] - j\left[\frac{\sigma_0}{\omega\epsilon_0(1+\omega^2\tau^2)}\right] \quad (11)$$

where ϵ_{rl}' is the dielectric constant associated with the carrier free sample, σ_0 ($= ne\mu$, μ is the carrier mobility) is the dc conductivity in the dark, and ω is the angular frequency of the EM wave. When the sample is illuminated, the dc conductivity becomes $\sigma_0 + \Delta\sigma$. The increment in conductivity $\Delta\sigma$ will give rise to an illuminated complex permittivity ϵ_{ri}, which can be expressed as

$$\epsilon_{ri} = (\epsilon_r' + \Delta\epsilon_r') - j(\epsilon_r'' + \Delta\epsilon_r'') \quad (12)$$

where

$$\Delta\epsilon_r' = \frac{-\Delta\sigma\tau}{\epsilon_0(1+\omega^2\tau^2)} \quad (13)$$

and

$$\Delta\epsilon_r'' = \frac{\Delta\sigma}{\omega\epsilon_0(1+\omega^2\tau^2)}. \quad (14)$$

From (13) and (14), a simple expression to relate τ to $\Delta\epsilon_r'$ and $\Delta\epsilon_r''$ can be obtained as follows:

$$\tau = \frac{-\Delta\epsilon_r'}{\omega\Delta\epsilon_r''}. \quad (15)$$

III. Experimental

A. Sample and Holder Preparation

Silicon and germanium samples for the measurements were first cut from (111)-oriented single-crystal wafers using a wheel saw and then chemically cleaned to remove the contaminants on the surface. Two tellurium samples were chemically cut from a Czochralski-grown single crystal [15], [16]. The samples were then chemically polished to obtain flat surfaces ($(10\bar{1}0)$ plane) and finally cut into square plates with a dimension of about 1×1 cm^2. To conduct the microwave measurements, a section of waveguide (sample holder) with a quartz (for wavelengths from 0.4 to 2 μm) or a Kodak IRTRAN 2 (for wavelengths from 1 to 5 μm) window was designed and fabricated to accept the external illumination. The cleaned sample was placed in the sample holder, with the large plane parallel to the side wall of the waveguide for the measurements.

B. Microwave Measurements

The sample holder waveguide together with the inserted sample was then introduced in the sample channel of the bridge system shown in Fig. 1(a). The complex relative permittivity of the sample in the dark was first determined by measuring the phase shift and attenuation of the propagating EM wave due to the presence of the sample in the waveguide [17]. The waveguide section with the sample in it was then slowly cooled to about 100 K. To measure $\Delta E_e/E_s$ and $\Delta E_h/E_s$, a calibrated diode was used. During the measurements, the bridge was first balanced by adjusting the attenuator and phase shifter in the reference channel. The phase shifter was then adjusted to plus 90° for $\Delta E_h/E_s$ and subsequently to minus 90° for $\Delta E_e/E_s$ (see Fig. 1(a)).

The monochromatic light was obtained from a tungsten–halogen lamp (chopped at 86 Hz) with a Beckman model 2400 monochromator for the wavelength range between 0.4 and 2 μm and from a Nerst glower source combined with a Perkin Elmer model 13 spectrophotometer for the range from 1 to 5 μm. The light intensity was measured using a calibrated silicon detector for the range between 0.5 and 1.0 μm and an InSb detector (Judson Infrared Inc.) for the range between 1 and 5 μm.

The electric field magnitude change due to the chopped illumination was measured using a lock-in amplifier directly connected to the diode. The data obtained for both $\Delta E_h/E_s$ and $\Delta E_e/E_s$ was then used to calculate ΔA_s and $\Delta\phi_s$ and thus $\Delta\epsilon_r'$ and $\Delta\epsilon_r''$ using (2), (3), (9), and (10). Typical values of ΔA_s and $\Delta\phi_s$ are 0.01 dB and 0.015° for silicon samples under the monochromatic illumination intensity of about 100 μw/cm^2.

In the present experiment, effects of the nonuniformity of the excited carriers in the samples have not been considered. Therefore, the results calculated using the formulas described in Section II should be regarded as "average" $\Delta\epsilon_r'$ and $\Delta\epsilon_r''$ values, especially when the optical absorption coefficient is large.

IV. Results

The spectral variation of $\Delta\epsilon_r'/E_q$ and $\Delta\epsilon_r''/E_q$ with wavelengths between about 0.8 and 2.0 μm, measured at three different temperatures, is shown in Figs. 3 and 4 for the germanium sample No. 46. Here, E_q is the density of photon flux incident on the sample. It is seen that with a decrease of the temperature the maximum value of the response increases (for both $\Delta\epsilon_r'/E_q$ and $\Delta\epsilon_r''/E_q$) and the peak values shift towards shorter wavelengths.

Results of $\Delta\epsilon_r'/E_q$ and $\Delta\epsilon_r''/E_q$ for the silicon sample No. 34 are shown in Figs. 5 and 6 over a wavelength range

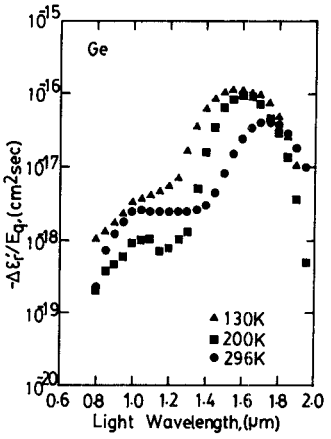

Fig. 3. $\Delta\epsilon_r'/E_q$ as a function of light wavelength for Ge.

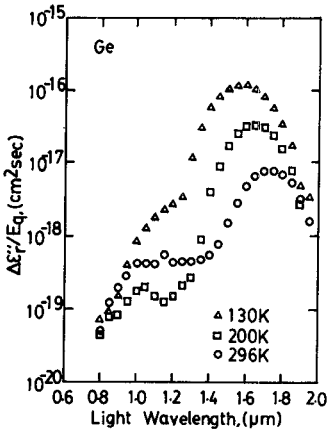

Fig. 4. $\Delta\epsilon_r''/E_q$ as a function of light wavelength for Ge.

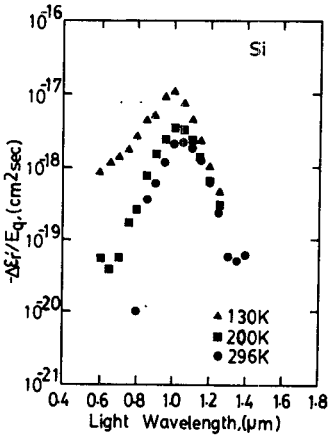

Fig. 5. $\Delta\epsilon_r'/E_q$ as a function of light wavelength for Si.

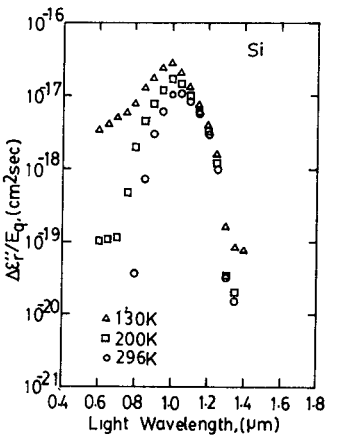

Fig. 6. $\Delta\epsilon_r''/E_q$ as a function of light wavelength for Si.

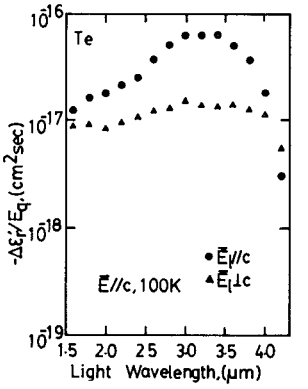

Fig. 7. $\Delta\epsilon_r'/E_q$ as a function of light wavelength for Te.

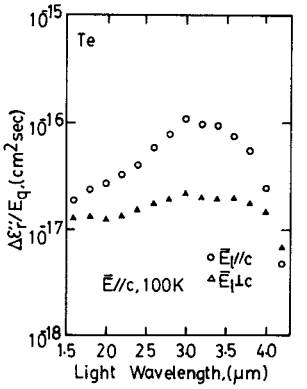

Fig. 8. $\Delta\epsilon_r''/E_q$ as a function of light wavelength for Te.

between about 0.6 and 1.4 μm. As the temperature decreases, the maximum value of the response again increases and the peak values shift slightly towards the shorter wavelength.

The results for a tellurium sample at 100 K are shown in Figs. 7 and 8 for $\boldsymbol{E}//c$ (here $\boldsymbol{E}$ is the electric field vector of the EM wave). It is seen that the response values for $\boldsymbol{E}_l//c$ ($\boldsymbol{E}_l$ is the electric field vector of the polarized incident light) are generally larger than those for $\boldsymbol{E}_l \perp c$ (c is the c-axis of tellurium crystal).

The relative change of $\Delta\epsilon_r'/E_{qm}$ and $\Delta\epsilon_r''/E_{qm}$ (E_{qm} is the photon flux density at the maximum intensity) for the germanium sample at different temperatures is plotted against the relative light intensity at a wavelength of 1.7 μm in Figs. 9 and 10, at a wavelength of 1.0 μm for the silicon sample in Figs. 11 and 12, and Fig. 13 for the tellurium sample at 3.6 μm. It is seen that the variation is almost linear in the log–log scales for all cases.

From the value of $\Delta\epsilon_r'$ and $\Delta\epsilon_r''$, the collision time τ can be calculated from (15). Such calculation was made for all the three samples using the intensity variation results shown

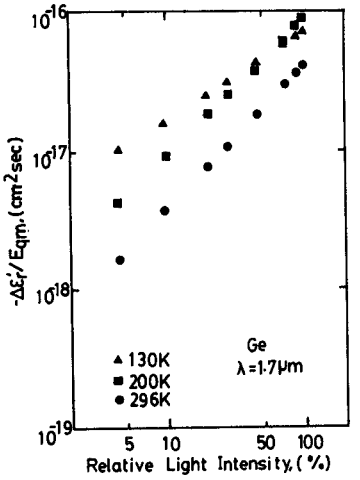

Fig. 9. $\Delta\epsilon_r'/E_{qm}$ as a function of light intensity for Ge.

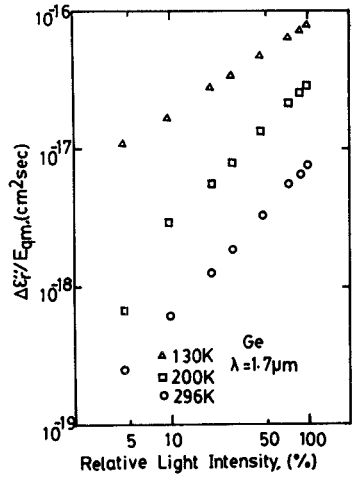

Fig. 10. $\Delta\epsilon_r''/E_{qm}$ as a function of light intensity for Ge.

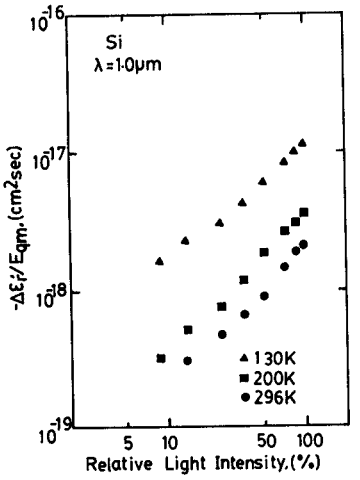

Fig. 11. $\Delta\epsilon_r'/E_{qm}$ as a function of light intensity for Si.

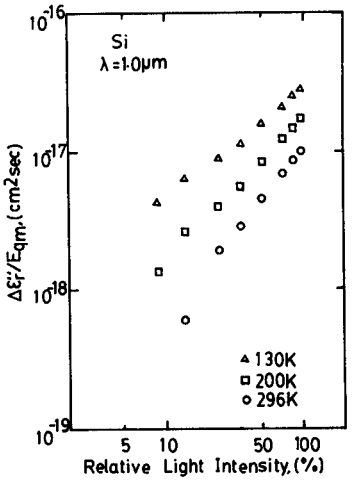

Fig. 12. $\Delta\epsilon_r''/E_{qm}$ as a function of light intensity for Si.

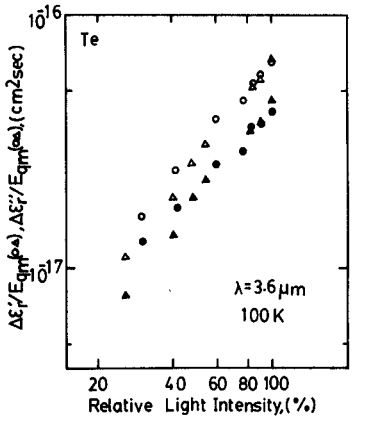

Fig. 13. $\Delta\epsilon_r'/E_{qm}$ and $\Delta\epsilon_r''/E_{qm}$ as a function of light intensity for Te (●⊙ $E_l//c$, ▲△ $E_l \perp c$).

TABLE I
COLLISION TIME RESULTS DERIVED FROM THE PHOTO-INDUCED PERMITTIVITY DATA

Sample No.	Length ℓ (cm)	Thickness d (cm)	Temperature T (K)	Optical* wavelength, λ,(μm)	$\frac{\Delta\epsilon_r'}{\Delta\epsilon_r''}$	τ (10^{-11}sec)	Reference τ-value (10^{-11}sec)
Si-33+	0.95	0.10	130	1.0	0.39	0.66	1.4 [18]
Ge-46++	0.67	0.11	130	1.7	0.91	1.55	1.3 [18]
Te-85**	1.05	0.10	100	3.6	0.66	1.25	0.22 [12]

*Light intensity about 100 μw/cm^2.
**$E \perp c$ and $E_l//c$.
†Boron doped, nominal resistivity 200 Ω·cm.
††Indian doped, nominal resistivity 24 Ω·cm.

in Figs. 9–13. Average values obtained are listed in Table I. τ-values for *p*-type silicon and germanium samples measured by the method of harmonic mixing of microwaves [18] and for a tellurium sample by the temperature dependent complex permittivity measurements [12] are also included in the same table.

V. DISCUSSION AND CONCLUSIONS

In the present work, it has been demonstrated that both the photodielectric and photoelectric effects can be observed in silicon, germanium, and tellurium single-crystal samples at temperatures in the range from 100 to 300 K using a simple microwave bridge system. Such experiments require determination of a phase shift change in the order of 0.002° and an attenuation change in the order of 0.0005 dB (the estimated experimental error is about 30 percent in

this extreme case) of the EM wave propagating through the illuminated sample.

It should be emphasized that both the phase shift change and the attenuation change (not the absolute phase and attenuation) were measured under the modulated illumination at about 90 Hz to obtain the photoconductive and photodielectric effects. Accordingly, in the method used, a slight disturbance in the environmental conditions will not have a detrimental effect on the measured results. Furthermore, with absolute measurements, the existence of an optical window in the waveguide wall would affect both the unperturbed field (without sample) and the perturbed one (with sample) and thus the directly measured complex permittivity values. However, all the results measured are the changes due to the illumination of the perturbed fields, and, therefore, the effect of the optical window was not considered in the present work.

For both germanium and silicon, the maximum of the photo-response increases with the decrease of temperature. The shift towards a shorter wavelength of the photoresponse peaks with the decreasing temperature is consistent with the fact that the fundamental energy gaps for both silicon and germanium decrease with the decrease of the temperature [19]. The variation of the response with monochromatic light intensity is almost linear in a log–log scale for all the samples. It should be pointed out, because of the influence of surface recombination velocity, carrier mobility, carrier life-time, and carrier concentration, that the photoconductive and photodielectric maximum cannot be identified precisely with the energy gap. This is possible only with a proper knowledge of the actual parameters mentioned above.

By using the permittivity equations derived for a classical model assuming a constant carrier collision time, the present photo-induced permittivity experiments allow this time constant to be deduced for the semiconductor samples. The τ-value determination is independent of the absolute magnitude of the sample complex permittivity. Since the collision time τ is a complicated function of dopant concentration, material quality, type of dopant, and sample temperature, only a qualitative comparison between the measured τ-values and that reported in the literature is possible. In order to make a quantitative comparison, it is required to obtain data using different methods on the same samples.

The effect of nonuniformity of the photo-generated carriers in the sample on the calculated results has not been considered in the present study. The nonuniformity will affect the calculated photo-induced complex permittivity results of the sample especially in the strong absorption region. More work is therefore needed in the future to take into consideration the nonuniformity effect.

References

[1] Yu. A. Cherkasov and L. N. Ionov, *Sov. Phys.—Solid State*, vol. 9, p. 722, 1967.

[2] L. N. Ionov, I. A. Akimov, and A. A. N. Terenin, *Sov. Phys.—Dokl.*, vol. 11, p. 599, 1967.

[3] K. Kalikstein, B. Kramer, and S. Gelfman, *J. Appl. Phys.*, vol. 39, p. 4252, 1968.

[4] S. S. Collier, A. A. Weiss, and R. F. Reithel, *Photogr. Sci. Eng.*, vol. 20, p. 54, 1976.

[5] R. H. Bube, *Photoconductivity of Solids*. New York: Wiley, 1960.

[6] E. E. Godik, *Sov. Phys.—Solid State*, vol. 18, p. 343, 1976.

[7] C. H. Lee, P. S. Mak, and A. P. DeFonzo, *IEEE J. Quantum Electron.*, vol. QE-16, p. 277, 1980.

[8] A. M. Johnson and D. H. Auston, *IEEE J. Quantum Electron.*, vol. QE-11, p. 283, 1975.

[9] L. N. Ionov, *Instrum. Exp. Tech.*, vol. 14, p. 1132, 1971.

[10] T. S. Benedict and W. Shockley, *Phys. Rev.*, vol. 89, p. 1152, 1953.

[11] T. S. Benedict, *Phys. Rev.*, vol. 91, p. 1565, 1953.

[12] P. Grosse and B. Krahl-Urban, *Phys. Stat. Sol.*, vol. 27, p. K149, 1968.

[13] I. Shih, L. Ding, S. Jatar, T. J. F. Pavlasek, and C. H. Champness, *IEEE Trans. Instrum. Meas.*, vol. IM-32, no. 2, pp. 326–331, June 1983.

[14] R. F. Harrington, *Time-Harmonic Electromagnetic Fields*. New York: McGraw-Hill, 1961, p. 317.

[15] M. El-Azab, C. R. McLaughlin, and C. H. Champness, *J. Cryst. Growth*, vol. 28, p. 1, 1975.

[16] I. Shih, and C. H. Champness, *J. Cryst. Growth*, vol. 44, p. 492, 1978.

[17] G. Nimtz, R. Dornhaus, M. Schifferdecker, I. Shih, and E. Tyssen, *J. Phys. E: Sci. Instrum.*, vol. 11, p. 1109, 1978.

[18] K. Seeger and K. Hess, *Z. Physik*, vol. 218, p. 431, 1969.

[19] S. M. Sze, *Physics of Semiconductor Devices*, 2nd ed. New York: Wiley, 1981.

Li Ding (M'83) was born in Shanghai, People's Republic of China, on November 29, 1937. He graduated from Qing-Hua University, China, in 1961.

From 1961 to 1981, he was a Lecturer in Chongqing University, China, teaching electromagnetic theory and microwave theory and techniques. Since March 1981, he has been a Visiting Scholar in the Department of Electrical Engineering at McGill University, Montreal, Quebec, Canada, where he has been engaged in research on microwave measurements. His interests are in electromagnetic theory, computers, microwave circuit design and measurement, microwave devices, and microwave IC's.

I. Shih was born in Taiwan, the Republic of China, in July, 1951. He received the B.S.E.E. degree from Cheng Kung University in 1973.

From 1973 to 1975, he was an officer in the Chinese Army. He joined the Electrical Engineering Department, McGill University, Montreal, Quebec, Canada, in 1975 and received the M.Eng. and Ph.D. degrees in 1977 and 1981, respectively. From 1981 to 1982, he was an NSERC Postdoctoral Fellow. He is now an NSERC Fellow at McGill University. His current technical interests include semiconductor materials preparation and characterization, semiconductor devices, and microwave measurements.

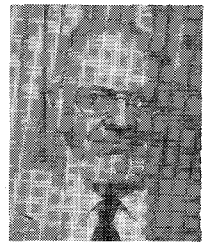

Thomas J. F. Pavlasek (SM'62) was born in London, England, in July 1923. He received the B.Eng., M.Eng., and Ph.D. degrees from McGill University, Montreal, Quebec, Canada.

He worked as a Design Engineer at RCA Canada and subsequently was a Research Associate at the Eaton Electronics Laboratory. He is a Professor in Electrical Engineering Department at McGill University, where he has taught since 1948. He is also Associate Dean for Planning and Development of the Faculty. His research interests are in microwave optics, EM wave scattering, near field measurements, antenna design techniques, and EM susceptibility problems.

Dr. Pavlasek in the Founding President of the Canadian Society for Electrical Engineering.

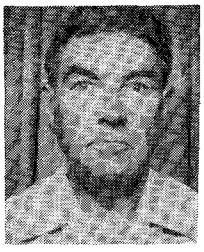

Clifford H. Champness was born in Surrey, England, in 1926. He received the B.Sc. in physics from the Imperial College of Science and Technology, in 1950, and was an exchange student in Eidgenossische Technische Hochschule, Zurich, in 1950–1951. He obtained the M.Sc. degree from the University of London, in 1957, and the Ph.D. degree from McGill University, Montreal, Quebec, Canada, in 1962.

From 1942–1947, he worked as an Assistant Experimental Officer on weapons development at the UK Ministry of Supply. As a Research Physicist at Associated Electrical Industries in Manchester, he investigated the transport properties of titanium dioxide, *III–V* compounds (mainly InAs and InSb), and treated the statistics of divalent impurity centers. From 1957–1960, he worked on silicon as a member of the Scientific Staff of the Research and Development Division of Northern Electric in Montreal. He was head of the Electronic Materials Department at the Noranda Research Centre, Pointe Claire, Quebec, from 1962–1967, where he directed work on thermoelectric cooling alloys based on bismuth telluride, epitaxial selenium film studies, and crystallization from amorphous selenium. In 1968, he was engaged as an Associate Professor by the Electrical Engineering Department of McGill University, where he has carried out research on the electronic and optical properties of selenium and tellurium. He was made full Professor in 1981. He has published over 50 papers on semiconductors, holds one patent, is a fellow of the former Physical Society of London, a member of the Canadian Association of Physicists, and a member of the American Physical Society.

An Analysis of an Electronically Tunable n-GaAs Distributed Oscillator

ASUO AISHIMA AND YOSHIFUMI FUKUSHIMA

Abstract—**The effective Schottky-barrier height of a contact to n-GaAs can be designed arbitrarily by interposing a thin, highly doped layer between a metal and n-GaAs and by controlling the thickness optimally. An n-GaAs diode with a Schottky-barrier cathode exhibits various space-charge modes depending on the barrier height. A traveling dipole domain mode in an n-GaAs diode changes into a cathode trapped domain mode as the injection current at the cathode decreases. It has been shown that an n-GaAs diode, which operates in a cathode trapped domain mode, exhibits a negative conductance over a fairly wide frequency range. A super wide-band electronically tunable distributed oscillator can be achieved by inserting an n-GaAs diode with a suitably designed Schottky-barrier cathode between resonant microstriplines in place of conventional dielectric material. It has been shown that the frequency of the distributed oscillator would be electronically tunable over a fairly wide frequency range from 9 to 26 GHz.**

NOMENCLATURE

$V(x)$	Potential in the diode.
q	Electronic charge.
ϵ	Permittivity.
N_L	Donor density in the active layer.
N_H	Donor density in the highly doped layer.
W	Length of the highly doped layer.
L	Length of the high-field layer in the active region.
V	Applied voltage.
Ψ	Wave function of electron.
m^*	Effective mass of the electrons in n-GaAs.
ζ	Eigenvalue of energy.
J_S	Current traversing from semiconductor to metal.
J_M	Current traversing from metal to semiconductor.
ϕ_{B0}	Work function in metal.
$\Delta\phi$	Barrier lowering due to image force.
T	Lattice temperature.
F_S	Fermi-Dirac distribution function in semiconductor.
F_M	Fermi-Dirac distribution function in metal.
E_d	Electric field at n^+–n interface.
$T(\eta)$	Transmission coefficient of electron.
ϕ_n	Potential difference between the Fermi level and the bottom of conduction band in GaAs.
A^*	Effective Richardson constant.
$n(x,t)$	Electron density.
$J(x,t)$	Conduction current density.
$E(x,t)$	Electric field.
$v(x,t)$	Electron velocity.
n_d	Donor density.
D_0	Diffusion constant of electron.
ω	Angular frequency.
$\tilde{n}(x,\omega)$	Small signal electron density.
$\tilde{J}(x,\omega)$	Small signal conduction current.
$\tilde{E}(x,\omega)$	Small signal electric field.
$\tilde{v}(x,\omega)$	Small signal electron velocity.
$\tilde{K}(x,\omega)$	Small signal total current.
$\tilde{\mu}(x,\omega)$	Differential mobility.
α, β, k	Propagation constant.
l	Length of the high-field layer in the active region.
l_1	Length of the low-field layer in the active region.

Manuscript received June 21, 1983; revised October 7, 1983.

The authors are with the Department of Electronics Engineering, Hiroshima University, Shitami, Saijohcho, Higashi-Hiroshima, 724 Japan.

0018-9480/84/0200-0157$01.00 ©1984 IEEE